Robust Under-Frequency Load Shedding With Electric Vehicles Under Wind Power and Commute Uncertainties

Hui Liu, *Senior Member, IEEE*, Houlin Pan, Ni Wang, Muhammad Zain Yousaf, Hui Hwang Goh, *Senior Member, IEEE*, and Saifur Rahman, *Life Fellow, IEEE*

***Abstract*—Under-frequency load shedding (UFLS) is an important measure for tackling low-frequency events caused by load-generation imbalance. However, the uncertainty of wind power amplifies power imbalances and can potentially impair frequency stability. Electric vehicles (EVs) present a more effective means for addressing this issue compared to load shedding. However, EVs have several limitations such as commute randomness. To ensure frequency stability and simultaneously reduce load shedding, a bi-level confidence-interval-based optimal strategy is proposed to enable the participation of EVs in UFLS, where the uncertainties of wind power and the commute randomness of EVs are estimated using a non-parametric kernel density estimation (KDE) method. In bi-level optimization, the upper level reduces the dependency on commute randomness and the wind power uncertainty during load-shedding events. Further, the upper-level solutions are sent to EV charging stations for emergency dispatch. By contrast, at the lower level, an approximation-function-based priority is proposed to optimize the task allocation. Simulation results show the advantages of the proposed approach in maintaining a stable frequency compared with traditional and adaptive UFLS schemes.**

***Index Terms*—Electric vehicle, robust optimization, under-frequency load shedding, uncertainty estimation, wind power.**

NOMENCLATURE

Variable

l	The number of examples
b_{w}	Bandwidth
$\alpha,\ \beta$	Confidence index
$U^{\alpha}_{\mathrm{error}}$	Upper bound of wind power
$L^{\alpha}_{\mathrm{error}}$	Lower bound of wind power
ΔP_{Wind}	Wind power prediction error
$\boldsymbol{U}$	A cluster of uncertainty sets
$t_{\text{h-w}}$	Departure time from home to work
$t_{\text{w-h}}$	Return time from work to home
$\mu_{\text{h-w}}$	Expected value of departure time
$\mu_{\text{w-h}}$	Expected value of return time
$\sigma_{\text{h-w}}$	Standard deviation of departure time
$\sigma_{\text{w-h}}$	Standard deviation of return time
θ	Shape parameter of gamma distribution
δ	Scale parameter of gamma distribution
γ	Standard deviation of standardized normal distribution
k_{w}	Shape parameter of Weibull distribution
c_{w}	Scale parameter of Weibull distribution
ΔE^{i}_{t}	Variation of EVs' number of the i^{th} sampling at time t
J	Number of Monte Carlo simulations
$\Delta E^{\mathrm{EV}}_{t}$	Variation of EVs' number at time t
U^{β}_{t}	Upper bound of the variation of EVs' number at time t
L^{β}_{t}	Lower bound of the variation of EVs' number at time t
$\Delta N^{t}_{\mathrm{EV}}$	Unknown number variation of EVs
$P_{\min}$	Lower bound of EV power
$P_{\max}$	Upper bound of EV power
P^{EV}_{i}	The power of an EV
P_{Gen}	Generation power
P_{Wind}	Wind power
P_{Load}	Load power
P_{d}	Power deficiency
$P_{\mathrm{d}}\ \%$	A certain percentage of power deficiency
P_{shed}	Load shedding plan
ΔP_{EV}	EV power injection
H_i	Inertia constant of the i^{th} generator
f_i	System frequency
f_{n}	Nominal frequency
f_{c}	Frequency of the equivalent inertial center
ξ	Equivalent inertia constant of the system
ΔP_{Load}	Load shedding amount
$P^{m,k}_{\mathrm{EVCS}}$	Power of the k^{th} EV charging station for the m^{th} round
N_{EVCS}	Number of EV charging stations
$P^{k}_{\mathrm{min,EVCS}}$	Lower bound of the power of an EV charging station

Manuscript received 24 April 2021; revised 8 October 2021 and 12 January 2022; accepted 30 April 2022. Date of publication 9 May 2022; date of current version 23 August 2022. This work was supported in part by the National Natural Science Foundation of China under Grant 51977041; in part by the Natural Science Foundation for Distinguished Young Scholars of Guangxi under Grant 2018JJG160007; and in part by the Innovation Project of Guangxi Graduate Education under Grant YCSW2021030. Paper no. TSG-00648-2021. *(Corresponding author: Ni Wang.)*

Hui Liu, Houlin Pan, Ni Wang, Muhammad Zain Yousaf, and Hui Hwang Goh are with the School of Electrical Engineering, Guangxi University, Nanning 530004, China (e-mail: hughlh@gxu.edu.cn; 528072976@qq.com; w_n604@163.com; mzainy1@gmail.com; hhgoh@gxu.edu.cn).

Saifur Rahman is with the Advanced Research Institute, Virginia Tech, Arlington, VA 22203 USA (e-mail: srahman@vt.edu).

Color versions of one or more figures in this article are available at https://doi.org/10.1109/TSG.2022.3172726.

Digital Object Identifier 10.1109/TSG.2022.3172726

$P^{k}_{\max,\mathrm{EVCS}}$	Upper bound of the power of an EV charging station
SOC	State of charge of an EV
$P^{\mathrm{EV}}_{n,k,0}$	Initial power of the n^{th} EV before UFLS
T_{charge}	Charge time of charge
$T_{\mathrm{discharge}}$	Discharging of discharge
a, b, c	Weighted indices
Q_{soc}	Willingness index contributed by the SOC
Q_{Pcharge}	Willingness index contributed by the charge power
Q_{T}	Willingness index contributed by the charge time
Q_{EV}	Willingness index of an EV
$P^{\mathrm{EV}}_{n,k,\mathrm{m}}$	The n^{th} EV power in the m^{th} round of UFLS.

Function

f	Probability distribution function
K	Kernel function
F	Cumulative density function
F^{-1}	Quantile function
Γ	The gamma function
$c^{i}_{\mathrm{EV}}(t)$	The curve of EV number in the i^{th} simulation.

I. Introduction

OWING to increasing concerns about sustainable development and environmental pollution, renewable energy resources—such as wind power—are replacing non-renewable energy resources in modern power systems. However, the randomness and uncertainty of renewable energy resources interfere with the load-generation balance, thus increasing the risk of system instability. Ensuring frequency stability while considering the randomness and uncertainty of renewable energy sources is becoming a significant challenge to the safe operation of power systems. Under-frequency load shedding (UFLS) aims to ensure frequency stability for the safe operation of power systems. UFLS can deal with this problem by automatically tripping selected loads to prevent frequency collapse and has attracted considerable attention [1]–[3].

In general, implementing UFLS includes estimating the power deficiency and tripping selected loads [4]. The estimation of the power deficiency determines the amount of load to be shed [4]. Overestimation results in unnecessary load shedding, while underestimation leads to unacceptable frequency deviations. The key to achieving better performance during UFLS is the accurate estimation of power deficiency. Therefore, the rate of change of frequency [5]–[7], second derivative of frequency [8], and gradient techniques [9] were investigated to assess power shortages. In [5], an equivalent inertial center was used to improve estimation accuracy while considering the rate of change of frequency. The swing equation of the generator was used to estimate the power deficiency [10]. In [11], the swing equation, ramp-up limit, and the rated capacity of generators were employed to support an appropriate power deficit estimation.

Attempts to improve approaches of power deficit estimation have been paid much attention to. In particular, the uncertainty in renewable energy generation such as distributed generation can affect the power imbalance estimations [12]–[14] and even causes severe system instability under extreme situations such as blizzards or heavy snow. Prior attempts have been made to cope with this issue. For instance, in [12], a power deficiency was estimated based on the frequency derivative in each shedding round to consider the influence of renewable energy generation. Reference [13] used the Markov model to calculate the outage probability of renewable energy generation, but this model may trigger an unnecessary load shedding while there exists no renewable generation loss. In [14], a probabilistic UFLS method is proposed to consider the uncertainties of system parameters including the uncertainties of inertia time constant, load damping, and distributed generation deficiency. An optimal robust UFLS scheme is proposed to shed the minimum load [15], where a scenario reduction algorithm is used to reduce the uncertainties caused by the generation deficiency of generators, variations in renewable energy resources, etc. Therefore, considering the probability of renewable energy generation loss has become an effective way to deal with the uncertainties during UFLS. In reality, an increase in renewable energy generation due to its uncertainty has also a significant influence on UFLS, as it can reduce the gap between load-generation imbalance during UFLS. If neglecting this influence, the UFLS strategy will result in unnecessary load shedding. However, few attentions are paid to this point.

Tripping selected loads is another concern that has been extensively addressed in the literature. Most researchers have focused on more appropriate locations and less load shedding [16]–[18]. For instance, an advanced load model related to voltage has been proposed to select where and how to shed loads instead of using an impedance model [7], but the load model imprecisely depicted the real load. The authors of [16] investigated a multiport network-based model to quickly search for the appropriate size and location of load shedding by considering the transient voltage on branch lines. In [17], a power-sensitivity-based approach was proposed to reduce the computational burden. Meanwhile, many researchers have noticed an increased risk of voltage instability due to arbitrary load shedding. Reference [18] analyzed the relationship between transient voltages and loads, and power flow tracing was proposed to prevent voltage instability due to load shedding.

Moreover, new flexible loads have attracted the attention of researchers owing to their energy-storage characteristics. Consequently, avoiding load shedding is becoming possible through the use of battery energy-storage systems (BESSs), one of the many key factors in the future of the smart grid. In [19], the control scheme of BESSs was investigated to avoid unnecessary load shedding. In [20], the power injection of BESSs was employed as an ancillary service and activated before load shedding. However, the extensive use of BESSs is limited due to expensive investment, the low energy density and complex control [21], etc.

Distributed flexible loads were also investigated to provide power injection under contingencies. In [22], dispatches of smart refrigerators and water heaters were conducted for UFLS. However, the strict constraints of intelligent refrigerators and water heaters limit their usefulness for periods

of UFLS. For instance, during continuous load shedding, any sharp increase in indoor temperature caused by atmospheric temperature can easily result in user discomfort and complaints. Electric vehicles (EVs) are a type of distributed energy-storage system that can be employed for UFLS [23]. This is because the capacity for UFLS—that is, the deviation between real-time power and discharging limit for an EV—can be adjusted continuously. In particular, EVs can provide the strong power support for the power grid due to the fast increase of EVs' number in recent years, and thus the vehicle-to-grid technology is becoming an increasing attention worldwide.

In this study, we aimed to overcome power deficiency during UFLS by discharging selected EVs in the case of wind power and EV uncertainties. For wind power uncertainty, a wind power prediction technique—that is, the bidirectional long short-term memory (Bi-LSTM) method [24]—is employed; the prediction error is estimated using a non-parametric kernel density estimation (KDE) method [25]. Furthermore, an EV uncertainty that the users can spontaneously drive away from charging stations, thereby decreasing the discharging capacity, is considered; this uncertainty is addressed by employing the non-parametric KDE method. Subsequently, combined with the two modeling in wind power and EV uncertainties, a robust optimization strategy for UFLS is proposed. Furthermore, for appropriate discharging selection of EVs, a priority list technique is proposed to speculate users' preferences and identify EV discharging conditions. The contributions of this study are as follow.

- An optimal approach is proposed to coordinate load shedding and EVs to reduce the impact of wind power uncertainty on power balance in an emergency, considering wind power prediction, traffic network, EV travel behaviors, EV users' willingness, etc.
- An approximation function is proposed to express the priority of EVs in participating in UFLS, considering EVs' willingness, EV charging power, etc.
- A non-parametric KDE method without considering types of probability distribution is firstly used to model the impact of EV commuting randomness on UFLS.
- Comparisons with other existing methods verify the robustness and effectiveness of the proposed approach in performing UFLS.

The remainder of this paper is organized as follows. In Section II, the problem of EV dispatch for UFLS is described. In Section III, a bi-level optimization method is provided. Simulations and discussions are presented in Section IV. Finally, conclusions are presented in Section V.

II. Problem Descriptions

A. The Framework of UFLS With Wind Power and EVs

As shown in Fig. 1, a hierarchical framework on UFLS is proposed to consider wind power uncertainty and at the same time, reduce load shedding as much as possible. When a low-frequency event occurs, in the control center, the power deficit is calculated based on the system frequency from the phasor measurement unit (PMU), and at the same time, an intelligent algorithm is used to perform the robust dispatch considering

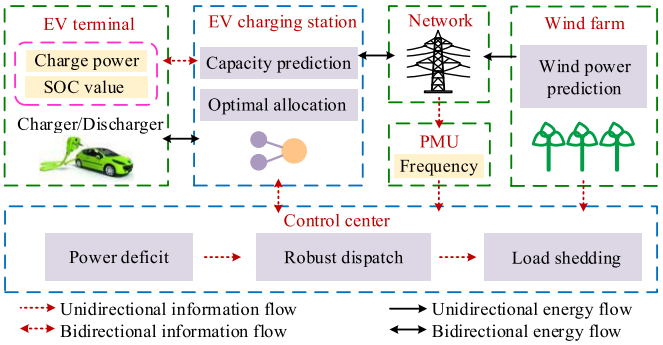

Fig. 1. The hierarchical framework of UFLS with wind power and EVs.

EV users' demands and wind power uncertainty. In addition, optimal solutions are sent to EV charging stations or dedicated relays in the system for load shedding.

In EV charging stations, the capacity of EVs is predicted and uploaded to the control center in real time, and the solution from the control center is optimally distributed between EVs based on their state of charge (SOC) and charging power.

B. The Impact of Wind Power Uncertainty on UFLS

While the frequency drops below the threshold value, UFLS will be activated to stop the frequency drop. However, wind power uncertainty has a significant impact on this action and may even harm the frequency stability owing to sudden changes in power deficiency [12], [26]. For instance, when wind power suddenly drops during UFLS, the gap between supply and the load will be amplified. In this condition, inappropriate power deficiency estimation will impact the frequency stability due to neglecting wind power uncertainty. Therefore, the influence of wind power uncertainty on UFLS must be compensated to ensure system frequency stability. This compensation is closely related to the prediction accuracy of wind power—that is, inaccurate prediction will increase frequency instability due to an inappropriate load shedding. Therefore, to ensure frequency stability under extremely adverse conditions, an appropriate robust method should be used to estimate the impact of wind power on UFLS while avoiding related risks.

C. The Uncertainty of the Capacity of EVs for UFLS

The capacity of an EV charging station is equal to the sum of the capacity of each EV at the station and is related to the number of connected EVs. For instance, while EVs drive away or do not take part in UFLS, the number of connected EVs will be reduced, and the capacity of EVs will decrease. Moreover, the randomness of EV users' actions—such as commuting and shopping—reduces the number of connected EVs, leading to a decrease in the capacity of EV charging stations. If the number of EVs decreases sharply and rapidly during UFLS, the power deficit is exacerbated, which can damage the frequency stability. Consequently, the impact of the uncertain capacity of EVs should be addressed, and an effective counteraction should be determined.

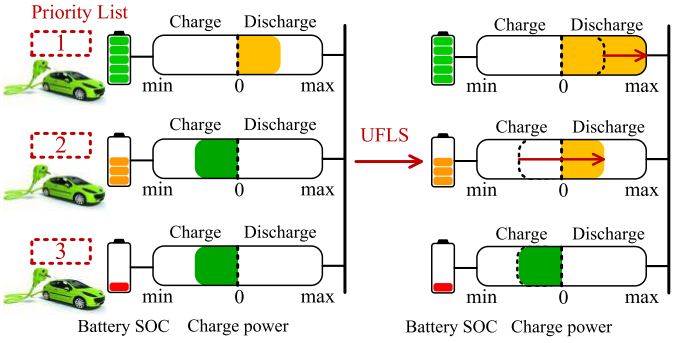

Fig. 2. Mechanism of the priority of EVs.

D. The Priority of EVs With User's Willingness

During a load-shedding task, EV charging stations classify EVs in a queue and then dispatch them in order. As shown in Fig. 2, the EVs at the top of the queue are fully discharged. This is because EV battery SOC levels are high enough for the next trip, and EV users would like to sell the redundant power to the power grid for revenue. The EVs enlisted second in the queue are not fully discharged, as EV uses would like to get the revenue, although battery SOC levels are not high enough. In some cases that EV battery energy cannot satisfy the next trip, these EVs will have the lowest priority in the queue and maintain charging. Therefore, the classification criteria for EVs are not only based on capacity, but also based on users' willingness. If any user chooses to sell EV-owned redundant power at a high SOC level, the EV should be placed at the front of the queue. To respond to UFLS and simultaneously consider users' willingness, EV charging stations should be authorized to determine their location in the queue. With this consideration, an approximation function will be proposed to describe users' willingness illustrated in Fig. 2. The function will rank EV users' priority according to EV SOC levels, charge power, etc.

III. Bi-Level Optimization for UFLS With Uncertainties of Wind Power and EVs

A. Uncertainty Modeling of Wind Power

A confidence-interval-based model is used to describe wind power uncertainty, which significantly reduces its impact on UFLS. While modeling, state-of-the-art methods–such as bidirectional long short-term memory (bi-LSTM) [24]–are used to predict wind power. At the same time, the non-parametric KDE method is used to model the prediction error [27], because it does not require any assumptions about the probability distribution function of the error.

For the non-parametric KDE technique, the Gaussian kernel function is commonly used and can consistently perform well in real-world scenarios [27]. Thus, we can obtain the f_{error} as (1):

$$f_{\text{error}}(\Delta P_{\text{Wind}}, b_{\text{w}}) = \frac{1}{\sqrt{2\pi} l b_{\text{w}}} \sum_{i=1}^{l} \exp\left(-\frac{1}{2}\left(\frac{\Delta P_{\text{Wind}} - E_i}{b_{\text{w}}}\right)^2\right) \tag{1}$$

Coherently, with the cumulative density function F_{error} and the quantile function F^{-1}_{error} are calculated, the upper and lower bounds with a confidence level of 1-α can be expressed as

$$\begin{cases} U^{\alpha}_{\text{error}} = F^{-1}_{\text{error}}(\alpha) \\ L^{\alpha}_{\text{error}} = F^{-1}_{\text{error}}\left(1 - \frac{\alpha}{2}\right) \\ \boldsymbol{U}\left\{\Delta P_{\text{Wind}} \middle| L^{\alpha}_{\text{error}} \le \Delta P_{\text{Wind}} \le U^{\alpha}_{\text{error}}\right\}. \end{cases} \tag{2}$$

B. Uncertainty Modeling of the Capacity of EVs

As the variation of connected EVs is greatly influenced by EV travel, a trip chain-based approach [29], [30] is considered to simulate their daily operation. The number and variation of EVs connected to the power grid are then modeled using a non-parametric KDE approach.

Based on the statistics from the U.K.'s 2016 National Travel Survey [31], the EV travel data is simulated using [32] as a reference. A typical trip chain in a day consists of the departure from the home (H), the work (W) in the morning, and arriving at howe (H) in the afternoon, which is abbreviated as H-W-H.

The return time $t_{\text{w-h}}$ and the initial departure time $t_{\text{h-w}}$ of H-W-H are fit with the standard distributions [33] and calculated as follows.

$$f(t; \mu, \sigma) = \frac{1}{\sigma\sqrt{2\pi}} \exp\left(-\frac{(t-\mu)^2}{2\sigma^2}\right) \tag{3}$$

Based on individual preferences, the departure time is different from EV to EV. Therefore, the Gamma distribution is used to fit the expected value of the departure time $\mu_{\text{h-w}}$, as shown in (4) [33].

$$f_{\text{Gamma}}(\mu_{\text{h-w}}; \delta, \theta) = \begin{cases} \frac{\theta^{-\delta}}{\Gamma(\delta)} \mu_{\text{h-w}}^{\delta-1} \exp\left(-\frac{\mu_{\text{h-w}}}{\theta}\right) & \mu_{\text{h-w}} \ge 0 \\ 0 & \mu_{\text{h-w}} < 0 \end{cases} \tag{4}$$

The standard deviation $\sigma_{\text{h-w}}$ fits the standardized normal distribution [33], and it is mathematically illustrated as

$$f_{\text{Norm}}(\sigma_{\text{h-w}}; \gamma) = \left| \frac{1}{\gamma\sqrt{2\pi}} \exp\left(-\frac{\sigma^2_{\text{h-w}}}{2\gamma^2}\right) \right| \tag{5}$$

The expected value of the return time μw-h sampled from the Weibull distribution is shown in (6) [33]:

$$f_{\text{Weibull}}(\mu_{\text{w-h}}; k_{\text{w}}, c_{\text{w}}) = \begin{cases} \left(\frac{k_{\text{w}}}{c_{\text{w}}}\right)\left(\frac{\mu_{\text{w-h}}}{k_{\text{w}}}\right)^{k_{\text{w}}-1} \exp\left(-\left(\frac{\mu_{\text{w-h}}}{c_{\text{w}}}\right)^{k_{\text{w}}}\right) & \mu_{\text{w-h}} \ge 0 \\ 0 & \mu_{\text{w-h}} < 0 \end{cases} \tag{6}$$

To include the change that EVs in different residential areas are with different travel behaviors, a traffic network topology with different speed limits of the road is employed [32]. Note that in the traffic network, the destinations of EVs are randomly sampled, and at the same time, the Dijkstra and Floyd-Warshall algorithm is used to guide the drive [34]. Considering the traffic jam, we can obtain information about the EV travel timetable, such as the arrival times at destinations. Therefore, we can calculate the number of EVs at each destination in a time step and obtain the $c_{\text{EV}}(t)$ curve of their variation. Assuming that every destination has a charging station, the $c_{\text{EV}}(t)$ curve is the description of the number of EVs at a charging station. Therefore, the variation in the number of EVs can be calculated using (7):

$$\Delta E^i_t = c^i_{\text{EV}}(t) - c^i_{\text{EV}}(t-1) \quad i = 1, \ldots, J \tag{7}$$

Using these conditions, the non-parametric KDE model is used to estimate the variation number of EVs to provide a probability distribution function using (8).

$$f_t^{\mathrm{EV}}\left(\Delta E_t^{\mathrm{EV}}, b_{\mathrm{w}}\right) = \frac{1}{\sqrt{2\pi} J b_{\mathrm{w}}} \sum_{i=1}^{J} \exp\left(-\frac{1}{2}\left(\frac{\Delta E_t^{\mathrm{EV}} - \Delta E_t^i}{b_{\mathrm{w}}}\right)^2\right) \tag{8}$$

The cumulative density function F_{EV} and the quantile function F_{EV}^{-1}can be used to evaluate the upper and lower bounds of the number variation of EVs at time t. By providing β, the upper and lower bounds with a confidence level of 1-β have the following expression.

$$\begin{cases} U_t^{\beta} = F_{\mathrm{EV}}^{-1}(\beta) \\ L_t^{\beta} = F_{\mathrm{EV}}^{-1}\left(1 - \frac{\beta}{2}\right) \\ L_{\mathrm{EV}}^{\beta} \le \Delta N_{\mathrm{EV}}^t \le U_{\mathrm{EV}}^{\beta} \end{cases} \tag{9}$$

For a charging station, the capacity variation of EVs at time t, a cluster of uncertainty set $\boldsymbol{U}$, is calculated based on the interval of the number variation, as in (10).

$$\boldsymbol{U}\left\{\Delta N_{\mathrm{EV}}^t \middle| P_{\min} L_{\mathrm{EV}}^{\beta} \le \sum_{i=1}^{\Delta N_{\mathrm{EV}}^t} P_i^{\mathrm{EV}} \le P_{\max} U_{\mathrm{EV}}^{\beta}\right\}. \tag{10}$$

C. Robust-Optimization-Based UFLS

While ignoring network losses, the generation and load are balanced, as

$$P_{\mathrm{Gen}} + P_{\mathrm{Wind}} = P_{\mathrm{Load}} \tag{11}$$

During an emergency, a power deficiency P_{d} is often calculated based on the frequency and the first-order time derivative, as described in (12) [12]. At the same time, a shedding plan P_{shed} must be implemented to ensure frequency stability, as shown in (13), which considers wind power fluctuation ΔP_{Wind} and EV injection ΔP_{EV}.

$$\begin{cases} P_{\mathrm{d}} = \sum P_{\mathrm{d},i} = \frac{2\sum H_i}{f_{\mathrm{n}}} \frac{\mathrm{d}f_{\mathrm{c}}}{\mathrm{d}t} = \xi \frac{\mathrm{d}f_{\mathrm{c}}}{\mathrm{d}t} \\ f_{\mathrm{c}} = \frac{\sum H_i f_i}{\sum H_i}, \xi = \frac{2}{f_{\mathrm{n}}} \sum H_i \end{cases} \tag{12}$$

$$\begin{cases} P_{\mathrm{d}} + P_{\mathrm{Gen}} + P_{\mathrm{Wind}} + \Delta P_{\mathrm{Wind}} = P_{\mathrm{Load}} + P_{\mathrm{shed}} \\ P_{\mathrm{shed}} = \Delta P_{\mathrm{Load}} + \Delta P_{\mathrm{EV}} \end{cases} \tag{13}$$

To minimize the load shedding ΔP_{Load}, we can set an objective function combined with (11) and (13). While considering the uncertainty of wind power and EVs, the objective is formed as a robust optimization, mathematically modeled as

$$\begin{cases} \max \min \Delta P_{\mathrm{Load}} \\ \quad = (\Delta P_{\mathrm{Wind}} + P_{\mathrm{d}} - \Delta P_{\mathrm{EV}}) \end{cases} \tag{14}$$

Furthermore, to maintain consistent power injection to the power system, the power of EV charging stations should be formed and limited, as in (15).

$$\begin{cases} \Delta P_{\mathrm{EV}} = \sum_{k=1}^{N_{\mathrm{EVCS}}} P_{\mathrm{EVCS}}^{m,k} - \sum_{k=1}^{N_{\mathrm{EVCS}}} P_{\mathrm{EVCS}}^{m-1,k} \\ P_{\mathrm{EVCS}}^{m,k} \le P_{\mathrm{EVCS}}^{m-1,k} \\ \sum_{i=1}^{\Delta N_{\mathrm{EV}}^t} P_i^{\mathrm{EV}} + P_{\mathrm{min,EVCS}}^k \le P_{\mathrm{EVCS}}^{m,k} \le P_{\mathrm{max,EVCS}}^k \\ \quad + \sum_{i=1}^{\Delta N_{\mathrm{EV}}^t} P_i^{\mathrm{EV}} \end{cases} \tag{15}$$

TABLE I
RELATIONSHIP BETWEEN CHARGE STATE AND QUEUE

Index of charge behavior	Variation	The seat in the priority list
SOC	+	↑
	-	↓
$P_{n,k,0}^{\mathrm{EV}}$	+	↓
	-	↑
T_{charge} /$T_{\mathrm{discharge}}$	T_{charge} /$T_{\mathrm{discharge}}$>1	↑
	T_{charge} /$T_{\mathrm{discharge}}$<1	↓

Note that in (15), the second constraint is used to conduct the behaviors of EV charging stations from charging to discharging, as the charging power is expressed with the positive number and the discharging power with the negative number. Combined with (2), (10), (14) and (15), the Robust-Optimization-based UFLS with EVs (RO-UFLS-EV) is proposed as (16). By solving (16), a tripping round of the shedding plan can be obtained.

$$\begin{cases} \max_{\Delta P_{\mathrm{Wind}}, \Delta N_{\mathrm{EV}}^t} \min_{P_{\mathrm{EVCS}}^{m,k}} \Delta P_{\mathrm{Load}} \\ \quad = \left(\Delta P_{\mathrm{Wind}} + P_{\mathrm{d}} - \sum_{k=1}^{N_{\mathrm{EVCS}}} P_{\mathrm{EVCS}}^{m,k} + \sum_{k=1}^{N_{\mathrm{EVCS}}} P_{\mathrm{EVCS}}^{m-1,k}\right) \\ \boldsymbol{U}\left\{\Delta P_{\mathrm{Wind}} \middle| L_{\mathrm{error}}^{\alpha} \le \Delta P_{\mathrm{Wind}} \le U_{\mathrm{error}}^{\alpha}\right\} \\ \boldsymbol{U}\left\{\Delta N_{\mathrm{EV}}^t \middle| P_{\min} L_{\mathrm{EV}}^{\beta} \le \sum_{i=1}^{\Delta N_{\mathrm{EV}}^t} P_i^{\mathrm{EV}} \le P_{\max} U_{\mathrm{EV}}^{\beta}\right\} \\ P_{\mathrm{EVCS}}^{m,k} \le P_{\mathrm{EVCS}}^{m-1,k} \\ \sum_{i=1}^{\Delta N_{\mathrm{EV}}^t} P_i^{\mathrm{EV}} + P_{\mathrm{min,EVCS}}^k \le P_{\mathrm{EVCS}}^{m,k} \le P_{\mathrm{max,EVCS}}^k \\ \quad + \sum_{i=1}^{\Delta N_{\mathrm{EV}}^t} P_i^{\mathrm{EV}}. \end{cases} \tag{16}$$

D. Priority Optimization of EVs

As discussed previously, the charging station ranks EVs based on users' preferences and EV charging conditions, called the priority list. While optimizing the priority list, scenarios such as the EV SOC and queue location are considered. For example, if the SOC of an EV is high, users will be able to sell redundant energy during UFLS. Meanwhile, if a random EV is charged before UFLS, it will remain charged during UFLS while waiting in the queue to be discharged. However, if the charging time is longer than the previous discharging time, the user will likely obtain a charging slot and not be discharged while waiting in the queue with the low priority, as illustrated in Table I.

Next, using (17)–(19), linear functions are investigated to formulate the relationships. Specifically, we assume that when the charging time is equal to the discharging time, the willingness index is assigned a value of 0.5, owing to the equivalent probability of charging or discharging.

$$\begin{cases} Q_{\mathrm{SOC}}(t) = SOC(t) \\ SOC(t) = SOC(t_0) + \frac{1}{C_{\mathrm{EV}}} \int_{t_0}^{t} P_{n,k,m}^{\mathrm{EV}} \mathrm{d}t \end{cases} \tag{17}$$

$$Q_{\mathrm{Pcharge}} = -0.5 P_{n,k,0}^{\mathrm{EV}} + 0.5 \tag{18}$$

$$Q_{\mathrm{T}} = \begin{cases} -0.5 \frac{T_{\mathrm{charge}}}{T_{\mathrm{discharge}}} + 1 & \frac{T_{\mathrm{charge}}}{T_{\mathrm{discharge}}} \le 1 \\ 0 & \frac{T_{\mathrm{charge}}}{T_{\mathrm{discharge}}} > 1 \end{cases} \tag{19}$$

$$Q_{\mathrm{EV}} = a Q_{\mathrm{SOC}} + b Q_{\mathrm{Pcharge}} + c Q_{\mathrm{T}} \tag{20}$$

Algorithm 1 RO-UFLS-EV for Multi-Machine Power Systems

a. Initialization: Confidence level 1-α. A set of the shedding threshold $F = \{f_{\mathrm{T}0}, \ldots, f_{\mathrm{T}m}, \ldots, f_{TM}\}$, which f_{Tm} is the m^{th} shedding threshold. M is the length of the threshold set. f_{n} is the rated frequency. Shedding round $m = 0$.

Main procedure:

b. Use bi-LSTM to predict wind power. Calculate and save the prediction error.

c. Update fluctuation interval of wind power by (1)–(2) using a confidence level of 1-α.

d. Load the variation interval of EV number from **Algorithm 2**.

e. Obtain system frequency f.

While $f \leq f_{\mathrm{T}m}$ do

f. Calculate the power deficit P_{d} by (12).

g. Solve the robust optimization-based UFLS (16). Send to EV charging station.

h. Shed loads ΔP_{Load}. Shedding round $m + 1$.

End

i. Return to step b.

Algorithm 2 Task Allocation in an EV Charging Station

a. Initialization: Confidence level 1-β. Shedding round $m = 0$.

Main procedure:

b. Update variation interval of EVs by (8)–(10) using a confidence level of 1-β. Send it to the **Algorithm 1**.

c. Monitor the data of EVs $P^{\mathrm{EV}}_{n,k,0}$, *soc*, T_{charge} and $T_{\mathrm{discharge}}$. Calculate Q_{EV} for each EV by (17)– (20).

While $f \leq f_{\mathrm{n}}$ do

d. Download dispatch task .

e. Solve the optimization (21) subjected to (22) and (23). Output the order $P^{\mathrm{EV}}_{n,k,m}$to EVs.

f. Shedding round $m + 1$.

End

As shown in (20), the function is the weighted sum of the SOC, charging power, and charging time. A reasonable priority list can be realized by calculating the willingness index Q_{EV} of the EVs and sorting them by size.

During an emergency, EV charging station waits for a dispatch from the control center. To allocate the dispatch to EVs with the priority, the objective in (20) is considered in EV charging stations. Subsequently, the EVs compensate for the power task by following (22). The dispatch power for EVs must be limited by the allowable power, as shown in (23). By solving the proposed programming, the dispatched power of each EV can be obtained.

$$\min \sum_{k=1}^{N_{\mathrm{EVCS}}} \sum_{n=1}^{N_k^{\mathrm{EV}}} Q_{\mathrm{EV}} \left(P^{\mathrm{EV}}_{n,k,0} - P^{\mathrm{EV}}_{n,k,m} \right) \tag{21}$$

$$\sum_{n=1}^{N_k^{\mathrm{EV}}} P^{\mathrm{EV}}_{n,k,m} = P^{m,k}_{\mathrm{EVCS}} \tag{22}$$

$$P_{\min} \leq P^{\mathrm{EV}}_{n,k,m} \leq P_{\max}. \tag{23}$$

E. The Proposed RO-UFLS-EV Algorithm

For clarity, the proposed algorithm—Algorithm 1—based on UFLS (RO-UFLS-EV) for multi-machine power systems and the proposed allocation algorithm—Algorithm 2—for the EV charging station are as follows.

Note that the proposed UFLS algorithm does not have an over-regulation impact on the system due to the conservative estimation of the power deficiency, although the so-called droop control method may result in an over-regulation impact while considering inappropriate droop coefficients [35], [36].

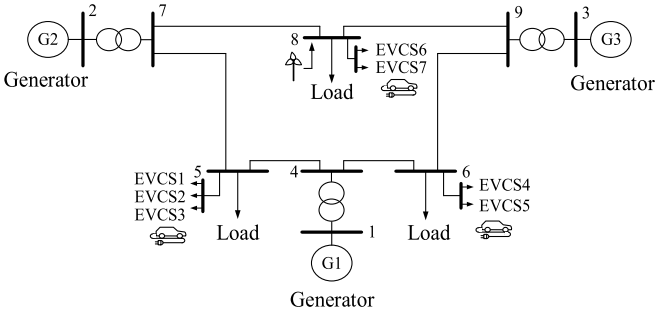

Fig. 3. An improved IEEE 9-bus power system.

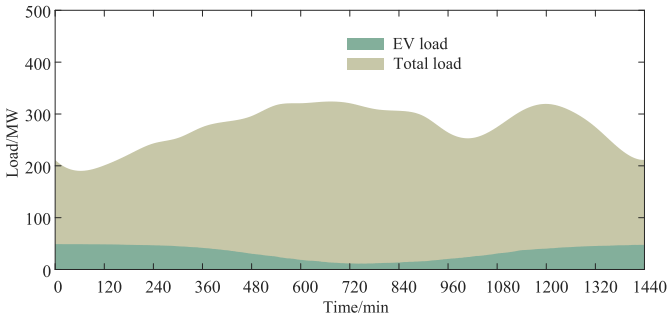

Fig. 4. The load level of the improved IEEE 9-bus power system.

IV. Numerical Simulation and Discussion

A. Simulation System

The proposed model is examined on an improved IEEE 3-machine 9-bus system illustrated in Fig. 3 with the load level shown in Fig. 4. The second-order synchronous generator model is used and simulated under the MATLAB/SIMULINK environment.

1) *Wind power parameter:* The wind farm is installed in Bus 8 with the rated power of 60 MW, the wind power of which is from a real wind farm located in Southwest China with the cut-in wind speed of 3 m/s and the cut-out wind speed of 20 m/s. To ensure prediction accuracy, we consider 7,200 data sets for training and 1,800 data sets for testing.

2) *EV parameters:* Three EV aggregators are considered in Buses 5, 6, and 8 with EV charging stations, as shown in Fig. 3, and every EV charging station has 1,000 EVs. Considering home charging stations, we assume that an EV has the maximum charging/ discharging power of 7 kW and the rated capacity of 32 kWh. The SOC levels and charging power of EVs are simulated by the Monte Carlo method [21]. The parameters of the daily commuting simulation are shown in Table II, and the traffic conditions can be found in [37].

3) *UFLS parameters:* The UFLS scheme usually consists of basic rounds and the special rounds, as illustrated in Table III. The detailed parameters include frequency thresholds, time delay, etc., which can also be found in [1].

B. The Uncertainties of EV Charging Stations

1) Commuting Uncertainty Estimation: A transport simulation is used to estimate the uncertainty of EVs, that is the

TABLE II
DAILY COMMUTING PARAMETERS

Type	Distribution	Parameter setting
H-W	$N(\mu_{\text{h-w}}, \sigma_{\text{h-w}})$	$\mu_{\text{h-w}} \sim Gamma\ (18.63, 28.14)$ $\sigma_{\text{h-w}} \sim N\ (0, 159.36)$
W-H	$N(\mu_{\text{w-h}}, \sigma_{\text{w-h}})$	$\mu_{\text{w-h}} \sim Weibull\ (1061.4, 8.63)$ $\sigma_{\text{w-h}} \sim N\ (158.45.91.17)$

TABLE III
THE PARAMETER SETTING OF UFLS

Round		Time delay /s	Shedding /P_d%	Threshold /Hz
Basic round	1	0.2	25	49.30
	2	0.2	25	49.10
	3	0.2	20	48.90
	4	0.2	15	48.70
	5	0.2	15	48.50
Special round	1	15	8	49.50
	2	20	8	49.50
	3	25	8	49.50

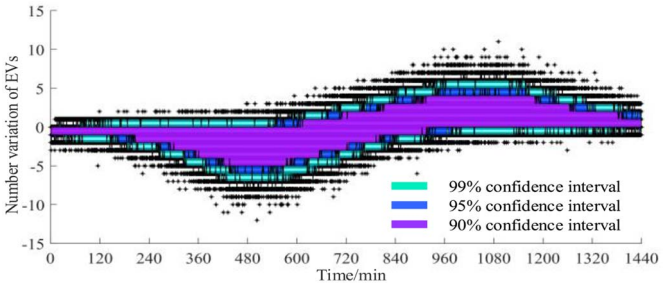

Fig. 5. Variation of EVs' number in an EV charging station with 1,000 EVs.

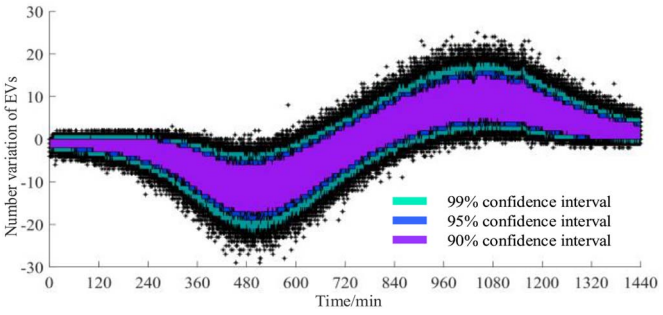

Fig. 6. Variation of EVs' number in an EV charging station with 2,000 EVs.

dynamic number of EVs at the charging points. The testing region containing 29 buses and 49 lines is classified into two residential districts and two office areas [32]. The starting and endpoint of each EV journey are selected randomly. Initially, 1000 or 2000 EVs are estimated at the charging station for test cases. The Monte Carlo method is used to simulate 5,000 times to estimate the EV variation at the charging points. The traffic conditions of the daily commuting simulation are referred to [37].

As shown in Figs. 6 and 7, the variation in EVs' number is marked in different colors for different confidence intervals. The number of EVs in a charging station varies with the time

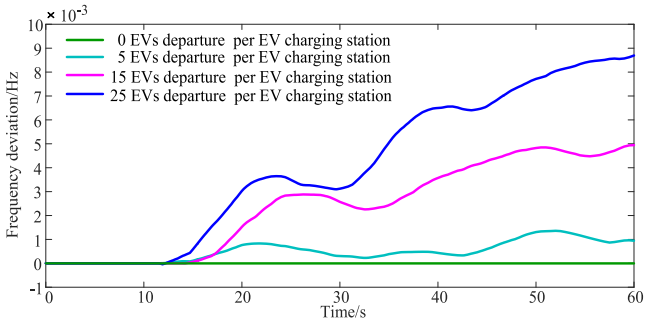

Fig. 7. Frequency deviation of different amount of departing EVs.

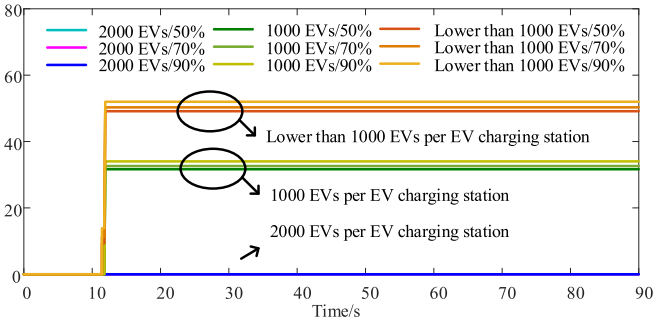

Fig. 8. Load shedding for different numbers of EVs considering generator trip.

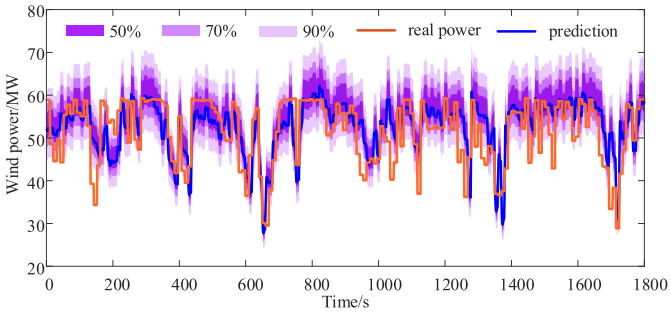

Fig. 9. A segment of wind power prediction and interval.

due to commuting randomness. For instance, during the morning or evening rush hours (i.e., around 480 min or 1080 min), the number of EVs in a charging station decreases due to leaving from the home, a.m., or returning the home, p.m. Therefore, the commuting uncertainty has a significant influence on the number of EVs in a charging station, and it will impact system frequency dynamics.

In order to analyze the influence of EVs leaving the station on the frequency deviation, we assume that at t = 10 s, the generator at Bus 3 is tripped with the power of 85 MW. In this condition, a larger frequency deviation will occur, when a higher number of EVs leaves the station, as shown in Fig. 7.

2) The Influence of EV Amount on Load Shedding: As shown in Fig. 9, using RO-UFLS-EV 50%, the load shedding is 31.43 MW considering 1,000 EVs in each charging station, while in the case of 2000 EVs per charging station, there is no load shedding.

While we randomly select the number below 1,000 of EVs for each charging station, the load shedding is 47.18 MW

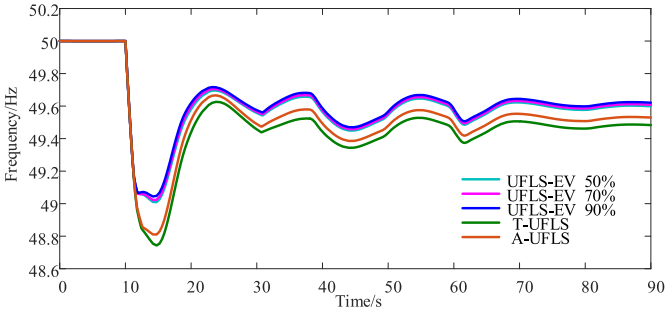

Fig. 10. Frequency response considering generator trip.

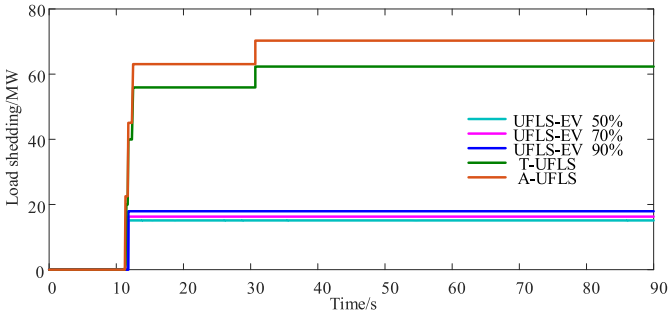

Fig. 11. Load shedding considering generator trip.

and is larger than that of 1,000 EVs in each charging station. Therefore, the increase of the number of EVs at the charging station can reduce the load shedding significantly.

C. The Prediction Conditions of Wind Power

In order to show the impact of wind power uncertainty on UFLS, we respectively consider the 50%, 70%, and 90% confidence interval of the prediction errors of wind power. As shown in Fig. 9, these different confidence intervals can show wind power uncertainty in different degrees, which means different impacts on the system. Therefore, they can be used to verify the effectiveness of the proposed approach in ensuring frequency stability.

D. Generator Trip

Frequency response performance: Traditional UFLS (T-UFLS), adaptive UFLS (A-UFLS), and the proposed UFLS (RO-UFLS-EV) model are compared in terms of frequency dynamic and the load shedding. With the 50%, 70%, and 90% confidence interval of the prediction errors of wind power, the proposed UFLS method is respectively marked as RO-UFLS-EV 50%, 70%, and 90% for simplification. While the generator connected to the bus-3 is tripped at $t = 10$ s, the power imbalance is 85 MW, which is approximately 26.59% of the current load. At the same time, wind power generation is reduced owing to uncertain wind speed, and the maximum generation loss is approximately 25 MW owing to wind farm variations. The power imbalance reaches approximately 110 MW.

As shown in Fig. 10, for T-UFLS, A-UFLS, RO-UFLS-EV 50%, RO-UFLS-EV 70%, and RO-UFLS-EV 90%, the frequency reaches the steady states of 49.48, 49.52, 49.60, 49.61, and 49.62 Hz, respectively. Therefore, the better performance is achieved by the proposed approach than T-UFLS and A-UFLS. With an increase of the confidence interval of wind power prediction, the proposed approach could ensure the steady state of the system frequency closer to the rated frequency (i.e., 50 Hz).

Under the T-UFLS mode, three tripping scenarios respectively occur at $t = 11.33$ s, $t = 11.71$ s, and $t = 12.41$ s, as shown in Fig. 11. This causes 19.97, 20, and 15.99 MW load-shedding events, respectively. Meanwhile, a special round produces at $t = 30.71$ s to achieve the frequency of above 49.5 Hz by the load-shedding event of 6.39 MW. Therefore, the total load shedding of T-UFLS reaches 62.33 MW. For the A-UFLS mode, the total load shedding reaches 68.67 MW, including the three tripping rounds implemented with 22.01 MW at $t = 11.40$ s, 22.01 MW at $t = 11.71$ s, and 17.6 MW at $t = 12.59$ s. A special round is also activated using 7.04 MW load shedding to elevate the frequency level, as in the previous case.

However, with EVs' participation, the amount of load shedding is reduced significantly. For example, as shown in Fig. 11, the proposed approach under the RO-UFLS-EV 50% mode only performs the load shedding of 15.11 MW, as the power of 56.64 MW is from EVs. Compared to the 68.67 MW and 62.33 MW load-shedding events under A-UFLS and T-UFLS modes, the total power of both the load shedding of 15.11 MW and the power of 56.64 MW from EVs is closer to the real power deficit of 110 MW. Because wind power uncertainty is considered in the proposed method, a more precise estimation of the power deficit may be realized.

As illustrated in Fig. 11, the RO-UFLS-EV 50% mode utilizes the load shedding of 15.11 MW, load shedding reaches 16.28 MW for the RO-UFLS-EV 70% mode, and in the RO-UFLS-EV 90% mode, the load shedding is 17.93 MW. Therefore, an increase in the confidence interval causes more load shedding, because high confidence intervals such as RO-UFLS-EV 70% and 90% tend to cover more wind power forecasting intervals. As shown in Fig. 10, the frequency dynamics of RO-UFLS-EV 50%, 70%, and 90% are similar, because the lower bounds of these confidence intervals are close to one another, i.e., 50% for 27.92 MW, 70% for 26.75 MW and 90% for 25.10 MW.

1) The Priority and SOC Levels of EVs: As shown in Table IV, willingness index (Q_{EV}), SOC, charging power ($P^{\mathrm{EV}}_{n,k,0}$), and EV ratio of $T_{\mathrm{charge/discharge}}$ can help to place EVs in the priority list. For example, the proposed algorithm places the 62$^{\mathrm{nd}}$ EV at the top of the priority list owing to its high Q_{EV} and SOC values. However, not all of these variables are proportional to each other. The Q_{EV} of the 925$^{\mathrm{th}}$ EV is 0.669, but its zero $P^{\mathrm{EV}}_{n,k,0}$ is placed in the middle of the priority list. Even though the 151$^{\mathrm{st}}$ EV with $Q_{\mathrm{EV}} = 0.667$ is still discharging, the long discharging time in the past limits its location in the queue. The proposed algorithm efficiently places EVs in the priority list by accounting for higher values of Q_{EV}, SOC, T_{charge} $T_{\mathrm{charge/discharge}}$, and lower values of $P^{\mathrm{EV}}_{n,k,0}$.

Although participating in UFLS will have a negative influence on EV battery SOC, this influence is marginal. As shown

TABLE IV
THE PRIORITY LIST AND CHARGING SITUATION OF EVS

Index No	Number of EV	Q_{EV}	SOC	$P^{EV}_{n,k,0}$	T_{charge}/ $T_{discharge}$
1	62	0.821	0.690	-1.818	1.781
2	94	0.820	0.702	-2.353	1.292
3	74	0.817	0.695	-6.108	1.914
...			...		
376	925	0.669	0.687	0	1.821
377	688	0.668	0.687	0	0.247
378	151	0.667	0.712	-3.612	0.920
...			...		
998	541	0.263	0.402	3.692	1.149
999	615	0.262	0.391	2.173	0.705
1000	444	0.260	0.411	3.528	0.611

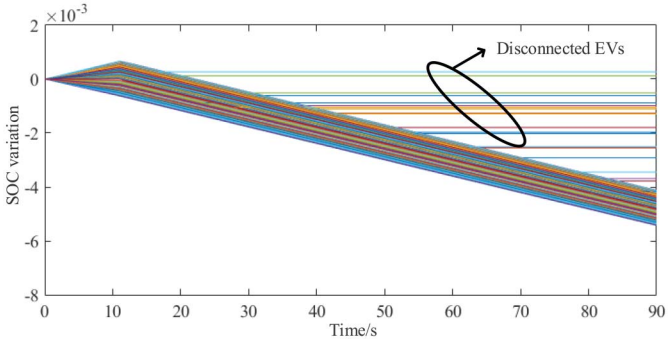

Fig. 12. The SOC variations of EVs considering generator trip.

TABLE V
THE COMPUTATION EFFICIENCY OF THE PROPOSED MODEL

Case	EV charging station			EVs in every	Calculation time /s	
	Bus 5	Bus 6	Bus 8	charging station	upper level	lower level
Case A	3	2	2	1000	0.031	0.016
Case B	30	20	20	1000	0.033	0.016
Case C	300	200	200	1000	0.163	0.016

TABLE VI
BIDIRECTIONAL COMMUNICATION TIME DELAY

Case	Time delay between the control center and charging stations /s	Time delay between charging station and EVs /s
Case A	0.1	0.1
Case B	0.2	0.2
Case C	0.3	0.3
Case D	0.4	0.4
Case E	0.5	0.5

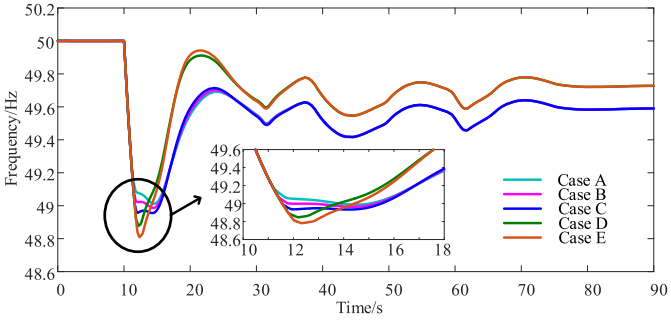

Fig. 13. The influence of time delay on frequency considering generator trip.

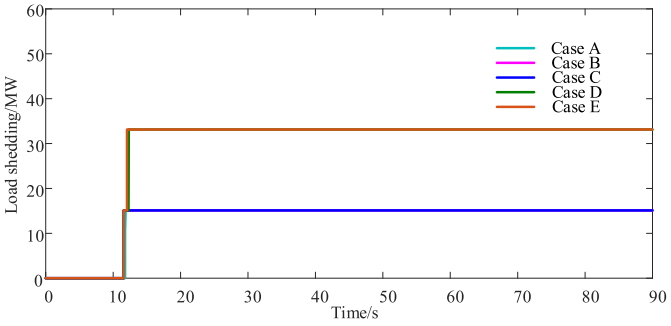

Fig. 14. The impact of time delay on load shedding considering generator trip.

in Fig. 12, the variation of EV SOC is about 0.5%, which means that the extended charging time is about 1.47 minutes while considering the charging power of 7 kW. On the other hand, if EVs drive away during UFLS, they will not be considered in the queue, as illustrated in Fig. 12.

2) Computation Complexity and Efficiency: The proposed method consists of upper-level model and the lower-level model. The upper-level model is for a robust linear optimization problem, and the lower-level model is for a linear optimization problem. Note that the robust problem can be transferred to a linear optimization problem by the duality theory. Therefore, the interior-point method with the polynomial convergence is here considered to high efficiently solve both linear optimization problems.

As illustrated in Table V, for the lower-level model solution, the proposed algorithm remains 0.016 s for three cases. This is because every EV charging station has the same number of EVs. Regarding the upper-level model solution, the calculation time will increase with the number of EV charging stations, but the computation is highly efficient. Note that we test the computation efficiency on an Intel Core i7 CPU 2.90 GHz Computer. A higher performance computer can improve the computation efficiency.

3) The influence of Time Delay on Frequency Dynamics: To discuss the influence of the communication time delay on system frequency dynamics, we consider three cases of the time delay, as illustrated in Table VI.

As shown in Fig. 13, for three cases illustrated in Table VI, the system has the lowest frequency of 49.01 Hz for Case A, 48.98 Hz for Case B, 48.94 Hz for Case C, 48.85 Hz for Case D, and 48.78 Hz for Case E, respectively. For Case A, B, and C, the frequency exceeds the threshold of 49.3 Hz and 49.1 Hz. Therefore, two basic rounds are needed. However, for Case D and E, an extra basic round is needed due to that the lowest frequency is below the load shedding threshold of 48.9 Hz, as shown in Figs. 13 and 14. In this condition, for Case D and E, the steady state frequency reaches 49.72 Hz, which is higher than the steady state frequencies for Case A, B, and C, as shown in Fig. 13.

Therefore, the time delay has a significant influence on the lowest frequency. In particular, the longer the time delay is,

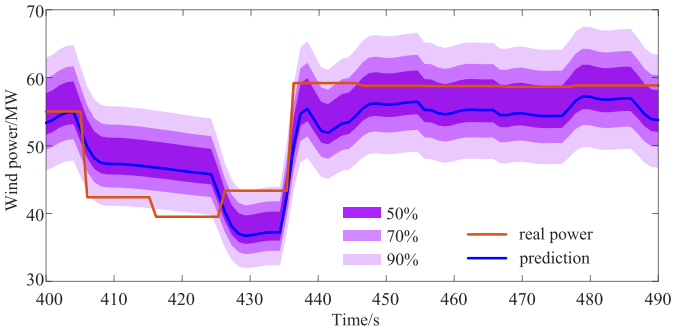

Fig. 15. Low prediction accuracy of wind power.

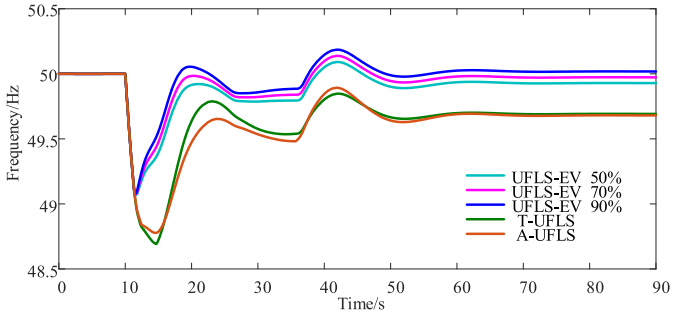

Fig. 16. System frequency under low prediction accuracy of wind power.

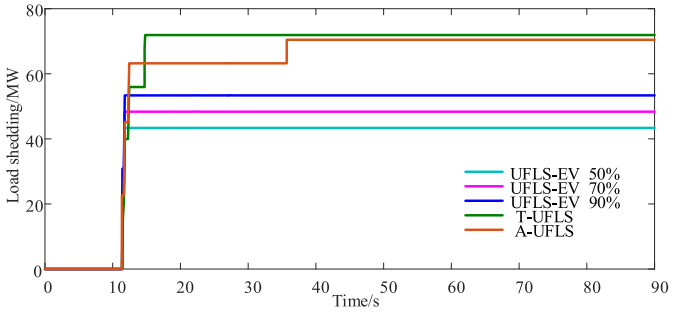

Fig. 17. Load shedding under low prediction accuracy of wind power.

the smaller the lowest frequency is, which may cause extra load shedding, as shown in Fig. 14.

4) Robustness Analysis: In order to discuss the robustness of the proposed method in ensuring system frequency, we considered the low prediction accuracy of wind power, as illustrated in Fig. 15.

As shown in Fig. 16, the frequency reaches the steady states of 49.69, 49.68, 49.92, 49.97, and 50.01 Hz for T-UFLS, A-UFLS, RO-UFLS-EV-50%, RO-UFLS-EV-70%, and RO-UFLS-EV-90%, respectively. The proposed method achieves more robust performance than T-UFLS and A-UFLS, even if different confidence intervals are considered for the low prediction accuracy of wind power.

At the same time, as shown in Fig. 17, the load removal reaches 71.92, 70.46, 43.37, 48.37, and 53.37 MW for T-UFLS, A-UFLS, RO-UFLS-EV-50%, RO-UFLS-EV-70%, and RO-UFLS-EV-90%, respectively. With an increase in the confidence interval, the load removal increases due to including more wind power forecasting intervals, and the proposed approach remains the more robust performance in reducing

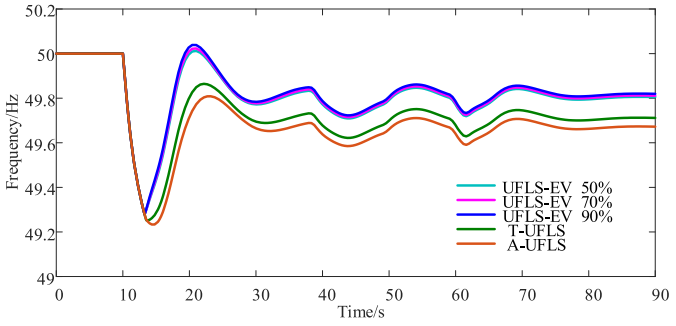

Fig. 18. Frequency response considering load increase.

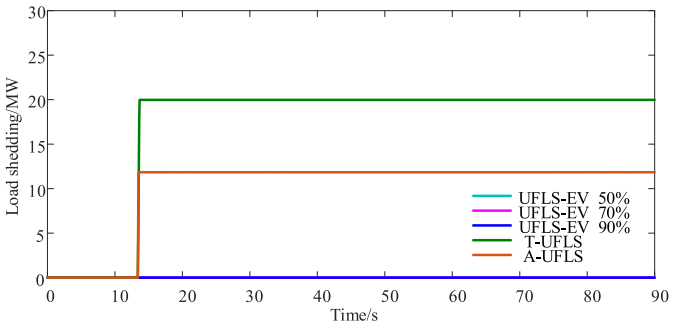

Fig. 19. Load shedding considering load increase.

load shedding, compared with T-UFLS and A-UFLS. This is because the proposed method is designed to withstand the worst wind power variance. The larger the wind power variance is, the more robust the system becomes.

Therefore, the confidence level of wind power prediction has a significant influence on the system. The proposed approach can remain good robust performance under different confidence levels. If considering a low risk of high frequency to obtain better performance in a low-frequency event, a middle- or low-confidence level should be suggested.

E. Load Increase

The load increases to 60 MW at $t = 10$ s, which is approximately 12.514% of the total load. With the wind power uncertainty, the total power imbalance of the system is 85 MW. As shown in Fig. 18, for T-UFLS, A-UFLS, RO-UFLS-EV-50%, RO-UFLS-EV-70%, and RO-UFLS-EV-90%, the frequency reaches the steady states of 49.71, 49.71, 49.67, 49.80, and 49.82 Hz, respectively. This means that the proposed method has the advantage in ensuring frequency stability over T-UFLS and A-UFLS.

As illustrated in Fig. 19, under the T-UFLS mode, a 19.97 MW load is cut off. Under the action of the A-UFLS mode, the power outage induces a load shedding of 11.85 MW. Under these circumstances, it is worth noting that employing EVs via the proposed model can fully compensate for the above load shedding to ensure the system frequency above 49.5 Hz, and thus there is no load shedding. Therefore, under the load increase scenario, ensuring frequency stability and no load-shedding events have shown the effectiveness of the proposed approach.

TABLE VII
COMPARISONS WITH EXISTING APPROACHES

Method	Wind power	Generator loss	Load increase	Flexible load	Time delay
[12], [38]	✓	✓	×	×	×
[14], [39]	×	✓	×	×	✓
[15]	✓	✓	✓	×	✓
[19]	×	✓	✓	✓	✓
[22]	×	×	✓	✓	✓
[23]	×	✓	✓	✓	✓
Proposed method	✓	✓	✓	✓	✓

F. Comparisons With Recent Works

The existing research has shown that the simulations, such as wind power uncertainty, generator trip, load increase, flexible load, and time delay, are important to validate the advantages of methods in performing UFLS. For instance, in [15], wind power, generator loss, load increase, and the time delay are considered; in [22], load increase, flexible load, and the time delay are addressed. However, most of the existing methods only consider part of these scenarios, in particular neglecting wind power uncertainty. By contrast, the proposed method includes more extensive scenarios, as illustrated in Table VII. Therefore, the proposed method is more realistic with a redundant approach.

V. CONCLUSION

This paper proposes a robust optimization of UFLS requirements to ensure frequency stability under various conditions. The wind power uncertainty and the commuting randomness of EVs are considered to be significant factors resulting in unexpected frequency drops. The non-parametric KDE method is adopted to estimate wind power and EV uncertainty, and a robust optimization-based model is proposed for extreme conditions. Numerical results demonstrated that the proposed approach can efficiently dispatch EVs with users' willingness and effectively suppress frequency deviations. Compared to T-UFLS and A-UFLS, the proposed approach can maintain higher frequency levels.

When applied to a real-world smart grid, a middle or lower value of the confidence level is suggested for a low risk of high frequency in a low-frequency event. Many factors, such as the reliability of communications, infrastructure, measurement conditions, and cyber-attacks, may affect the performance of the proposed model. Besides, the recharging of EVs may cause a significant second disturbance after UFLS. Therefore, our future work will focus on multi-stage load restoration plan of EVs during load recovery and evaluate the performance of the proposed method considering these factors mentioned above.

REFERENCES

[1] *IEEE Guide for the Application of Protective Relays Used for Abnormal Frequency Load Shedding and Restoration*, IEEE Standard C37.117-2007, Aug. 2007.

[2] B. Delfino, S. Massucco, A. Morini, P. Scalera, and F. Silvestro, "Implementation and comparison of different under frequency load-shedding schemes," in *Proc. PES Summer Meeting*, vol. 1, Jul. 2001, pp. 307–312.

[3] A. A. Girgis and W. L. Peterson, "Adaptive estimation of power system frequency deviation and its rate of change for calculating sudden power system overloads," *IEEE Trans. Power Del.*, vol. 5, no. 2, pp. 585–594, Apr. 1990.

[4] Y. Halevi and D. Kottick, "Optimization of load shedding system," *IEEE Trans. Energ. Convers.*, vol. 8, no. 2, pp. 207–213, Jun. 1993.

[5] V. V. Terzija, "Adaptive underfrequency load shedding based on the magnitude of the disturbance estimation," *IEEE Trans. Power Syst.*, vol. 21, no. 3, pp. 1260–1266, Aug. 2006.

[6] P. M. Anderson and M. Mirheydar, "An adaptive method for setting underfrequency load shedding relays," *IEEE Trans. Power Syst.*, vol. 7, no. 2, pp. 647–655, May 1992.

[7] U. Rudez and R. Mihalic, "Monitoring the first frequency derivative to improve adaptive underfrequency load-shedding schemes," *IEEE Trans. Power Syst.*, vol. 26, no. 2, pp. 839–846, May 2011.

[8] J. Jallad, S. Mekhilef, H. Mokhlis, and J. A. Laghari, "Improved UFLS with consideration of power deficit during shedding process and flexible load selection," *IET Renew. Power Gener.*, vol. 12, no. 5, pp. 565–575, Sep. 2018.

[9] U. Rudez and R. Mihalic, "Analysis of underfrequency load shedding using a frequency gradient," *IEEE Trans. Power Del.*, vol. 26, no. 2, pp. 565–575, Apr. 2011.

[10] S. Abdelwahid, A. Babiker, A. Eltom, and G. Kobet, "Hardware implementation of an automatic adaptive centralized underfrequency load shedding scheme," *IEEE Trans. Power Del.*, vol. 29, no. 6, pp. 2664–2673, Dec. 2014.

[11] Y. Tofis, S. Timotheou, and E. Kyriakides, "Minimal load shedding using the swing equation," *IEEE Trans. Power Syst.*, vol. 32, no. 3, pp. 2466–2467, May 2017.

[12] A. Ketabi and M. H. Fini, "An underfrequency load shedding scheme for hybrid and multiarea power systems," *IEEE Trans. Smart Grid*, vol. 6, no. 1, pp. 82–91, Jan. 2015.

[13] Y.-Y. Hong, M.-C. Hsiao, Y.-R. Chang, Y.-D. Lee, and H.-C. Huang, "Multiscenario underfrequency load shedding in a microgrid consisting of intermittent renewables," *IEEE Trans. Power Del.*, vol. 28, no. 3, pp. 1610–1617, Jul. 2013.

[14] T. Amraee, M. G. Darebaghi, A. Soroudi, and A. Keane, "Probabilistic under frequency load shedding considering RoCoF relays of distributed generators," *IEEE Trans. Power Syst.*, vol. 33, no. 4, pp. 2507–2515, Jul. 2018.

[15] A. Rafinia, J. Moshtagh, and N. Rezaei, "Stochastic optimal robust design of a new multi-stage under-frequency load shedding system considering renewable energy sources," *Int. J. Electr. Power Energy Syst.*, vol. 118, Jun. 2020, Art. no. 105735.

[16] Y. Wang, I. R. Pordanjani, W. Li, W. Xu, and E. Vaahedi, "Strategy to minimise the load shedding amount for voltage collapse prevention," *IET Gener. Transmiss. Distrib.*, vol. 5, no. 3, pp. 307–313, Mar. 2011.

[17] C. P. Reddy, S. Chakrabarti, and S. C. Srivastava, "A sensitivity-based method for under-frequency load-shedding," *IEEE Trans. Power Syst.*, vol. 29, no. 2, pp. 984–985, Mar. 2014.

[18] J. Tang, J. Liu, F. Ponci, and A. Monti, "Adaptive load shedding based on combined frequency and voltage stability assessment using synchrophasor measurements," *IEEE Trans. Power Syst.*, vol. 28, no. 2, pp. 2035–2047, May 2013.

[19] S. Pulendran and J. E. Tate, "Energy storage system control for prevention of transient under-frequency load shedding," *IEEE Trans. Smart Grid*, vol. 8, no. 2, pp. 927–936, Mar. 2017.

[20] C.-Y. Lai and C.-W. Liu, "A scheme to mitigate generation trip events by ancillary services considering minimal actions of UFLS," *IEEE Trans. Power Syst.*, vol. 35, no. 6, pp. 4815–4823, Nov. 2020.

[21] B. R. Chalamala, T. Soundappan, G. R. Fisher, M. R. Anstey, V. V. Viswanathan, and M. L. Perry, "Redox flow batteries: An engineering perspective," *Proc. IEEE*, vol. 102, no. 6, pp. 976–999, Jun. 2014.

[22] J. Wang, H. Zhang, and Y. Zhou, "Intelligent under frequency and under voltage load shedding method based on the active participation of smart appliances," *IEEE Trans. Smart Grid*, vol. 8, no. 1, pp. 353–361, Jan. 2017.

[23] H. Liu *et al.*, "Enabling strategies of electric vehicles for under frequency load shedding," *Appl. Energy*, vol. 228, pp. 843–851, Oct. 2018.

[24] H. Jahangir, H. Tayarani, S. S. Gougheri, M. A. Golkar, A. Ahmadian, and A. Elkamel, "Deep learning-based forecasting approach in smart grids with microclustering and bidirectional LSTM network," *IEEE Trans. Ind. Electron.*, vol. 68, no. 9, pp. 8298–8309, Sep. 2021.

[25] A. Majdara and S. Nooshabadi, "Nonparametric density estimation using copula transform, Bayesian sequential partitioning, and diffusion-based kernel estimator," *IEEE Trans. Knowl. Data Eng.*, vol. 32, no. 4, pp. 821–826, Apr. 2020.
[26] K. Samarakoon, J. Ekanayake, and N. Jenkins, "Investigation of domestic load control to provide primary frequency response using smart meters," *IEEE Trans. Smart Grid*, vol. 3, no. 1, pp. 282–292, Mar. 2012.
[27] B. Zhou, X. Ma, Y. Luo, and D. Yang, "Wind power prediction based on LSTM networks and nonparametric kernel density estimation," *IEEE Access*, vol. 7, pp. 165279–165292, 2019.
[28] N. Chao and F. You, "A data-driven multistage adaptive robust optimization framework for planning and scheduling under uncertainty," *AIChE J.*, vol. 63, no. 10, pp. 4343–4369, Aug. 2019.
[29] T. Shun, L. Kunyu, X. Xiangning, W. Jianfeng, Y. Yang, and Z. Jian, "Charging demand for electric vehicle based on stochastic analysis of trip chain," *IET Gener. Transmiss. Distrib.*, vol. 10, no. 11, pp. 2689–2698, Apr. 2016.
[30] S. J. Moura, J. L. Stein, and H. K. Fathy, "Battery-health conscious power management in plug-in hybrid electric vehicles via electrochemical modeling and stochastic control," *IEEE Trans. Control Syst. Technnol.*, vol. 21, no. 3, pp. 679–694, May 2013.
[31] "National Travel Survey: 2016." Gov. U.K. 2018. [Online]. Available: https://www.gov.uk/government/statistics/national-travel-survey-2016
[32] H. Li, Z. Du, L. Chen, and B. Zhou, "A spatial-temporal charging load forecasting modelling of electric vehicles considering urban traffic network," in *Proc. IEEE Innov. Smart Grid Technol. Asia (ISGT Asia)*, Singapore, 2018, pp. 127–132.
[33] F. Neumann, *Optimal Scheduling of Electric Vehicle Charging in Distribution Networks*. Edinburgh, Scotland: Univ. Edinburgh, 2017.
[34] Risald, A. E. Mirino, and Suyoto, "Best routes selection using Dijkstra and Floyd-Warshall algorithm," in *Proc. 11th Int. Conf. Inf. Commun. Technol. Syst. (ICTS)*, Surabaya, Indonesia, 2017, pp. 155–158.
[35] S. Izadkhast, P. Garcia-Gonzalez, P. Frías, and P. Bauer, "Design of plug-in electric vehicle's frequency-droop controller for primary frequency control and performance assessment," *IEEE Trans. Power Syst.*, vol. 32, no. 6, pp. 4241–4254, Nov. 2017.
[36] S. Izadkhast, P. Garcia-Gonzalez, and P. Frías, "An aggregate model of plug-in electric vehicles for primary frequency control," *IEEE Trans. Power Syst.*, vol. 30, no. 3, pp. 1475–1482, May 2015.
[37] Y. Shao *et al.*, "A spatial-temporal charging load forecast and impact analysis method for distribution network using EVs-traffic-distribution model," *Proc. CSEE*, vol. 37, no. 18, pp. 5207–5219, May 2017.
[38] Y.-Y. Hong and S.-F. Wei, "Multiobjective underfrequency load shedding in an autonomous system using hierarchical genetic algorithms," *IEEE Trans. Power Del.*, vol. 25, no. 3, pp. 1355–1362, Jul. 2010.
[39] F. Ceja-Gomez, S. S. Qadri, and F. D. Galiana, "Under-frequency load shedding via integer programming," *IEEE Trans. Power Syst.*, vol. 27, no. 3, pp. 1387–1394, Aug. 2012.

Hui Liu (Senior Member, IEEE) received the M.S. and Ph.D. degrees in electrical engineering from the College of Electrical Engineering, Guangxi University, China, in 2004 and 2007, respectively. He worked with Tsinghua University as a Postdoctoral Fellow from 2011 to 2013, and also with Jiangsu University as a Faculty Member from 2007 to 2016. He visited the Energy Systems Division, Argonne National Laboratory, Argonne, IL, USA, from 2014 to 2015. He joined the School of Electrical Engineering, Guangxi University in 2016, where he is a Professor and the Deputy Dean. His research interests include power system optimization, power system stability and control, electric vehicles, integrated energy systems, and demand response. He is an Editor of the IEEE TRANSACTIONS ON SMART GRID and the IEEE PES Letters. He is also an Associate Editor of the *IET Smart Grid* and the IET Generation, Transmission & Distribution.

Houlin Pan received the B.S. degree in electrical engineering from the South China University of Technology, Guangzhou, China, in 2019. He is currently pursuing the M.S. degree with the School of Electrical Engineering, Guangxi University, Guangxi, China. His research interests include power system optimization, electric vehicles, and frequency regulation.

Ni Wang received the M.S. degree in electrical engineering from Guangxi University, Nanning, China, in 2005, where she worked as a Faculty Member from 2005 to 2016. She joined the School of Electrical Engineering, Guangxi University in 2016. Her research interests include power system optimization, and power system stability and control.

Muhammad Zain Yousaf received the B.Eng. degree in electronics and electrical engineering from Swansea University, U.K., in 2014, and the M.Sc. degree in electrical engineering from The University of Lahore, Pakistan. He is currently pursuing the Ph.D. degree with the College of Electrical Engineering, Guangxi University, Guangxi, China. His research interests include power system optimization and control, and protection of multiterminal DC transmission systems.

Hui Hwang Goh (Senior Member, IEEE) received the B.Eng. (Hons.) and M.Eng. degrees in electrical engineering and the Ph.D. degree in electrical engineering from Universiti Teknologi Malaysia, Johor Bahru, Malaysia, in 1998, 2002, and 2007, respectively. He is currently a Professor of Electrical Engineering with the School of Electrical Engineering, Guangxi University, Nanning, China. He is also a Fellow of the Institution of Engineering and Technology, U.K., the ASEAN Academy of Engineering and Technology, and The Institution of Engineers, Malaysia, a Chartered Engineer under the Engineering Council United Kingdom, and a Professional Engineer under the Board of Engineers, Malaysia. His research interests include embedded power generation modeling and simulation, power quality studies, wavelet analysis, multicriteria decision making, renewable energies, and dynamic equivalent.

Saifur Rahman (Life Fellow, IEEE) is the Founding Director with the Advanced Research Institute, Virginia Tech, USA, where he is currently the J. R. Loring Professor of Electrical and Computer Engineering. He also directs the Center for Energy and the Global Environment. He has published over 140 journal papers and has over 400 conference and invited presentations. He is an IEEE Millennium Medal Winner. He was the Founding Editor-in-Chief of *IEEE Electrification Magazine* and the IEEE TRANSACTIONS ON SUSTAINABLE ENERGY. He served as the Chair of the U.S. National Science Foundation Advisory Committee for International Science and Engineering from 2010 to 2013. He is the President of the IEEE Power & Energy Society (PES) for 2018 and 2019. He is a Distinguished Lecturer for the PES and has lectured on renewable energy, energy efficiency, smart grid, energy Internet, blockchain, and IoT sensor integration in over 30 countries.